Proceedings of the 7th JFPS International
Symposium on Fluid Power, TOYAMA 2008
September 15-18, 2008

A COMPARISON OF AN AC-SERVO MOTOR DRIVING VARIABLE ROTATIONAL SPEED AND A VARIABLE DISPLACEMENT PUMP-CONTROLLED SYSTEMS FOR VELOCITY CONTROL

Mao-Hsiung CHIANG[1], Yih-Nan CHEN[1,3] and Chung-Chieh CHEN[2]

[1] Department of Engineering Science and Ocean Engineering,
National Taiwan University
106 Taipei, Taiwan
(E-mail: mhchiang@ntu.edu.tw)

[2] Graduate Institute of Automation and Control,
National Taiwan University of Science and Technology,
106 Taipei, Taiwan

[3] Department of Mechanical Engineering,
Tatung University
Taipei, Taiwan

ABSTRACT

In the hydraulic servo control applications, hydraulic valve-controlled systems, which have a problem of low energy efficiency, are used mostly because of the high response characteristics. Hydraulic pump-controlled servo systems have high energy-efficiency. However, the conventional pump-controlled systems, which are altered by displacement via variable displacement pumps, have lower response. This paper aims to investigate the servo performance of the high response and high energy efficiency electro-hydraulic pump-controlled system driven by a variable rotational speed AC servo motor in comparison with the conventional pump-controlled systems which are altered by displacement via variable displacement pumps. For that, the control strategy, adaptive fuzzy sliding-mode controller (AFSMC) is introduced. The AFSMC can not only simplify the fuzzy rule base but also estimate the equivalent control force and online self-tune the rule base through the adaptive strategy. The developed high response variable rotational speed electro-hydraulic pump-controlled system controlled by AFSMC and the conventional variable displacement pump-controlled system (VDPCS) are implemented and verified experimentally for velocity control with various velocity targets and external loading conditions. Furthermore, the energy efficiencies of different experiments are analyzed and compared precisely by the power quality recorder used to measure the electrical power consumed by the AC servo motor.

KEY WORDS

AC servo motor, Variable rotational speed, Variable displacement pump, Velocity control

INTRODUCTION

The present hydraulic systems are requested for both high response and high energy-efficiency. In view of the hydraulic circuits, two different hydraulic systems are classified, such as hydraulic valve-controlled system

and hydraulic pump-controlled system [1]. The hydraulic valve-controlled systems have high response but low energy-efficiency. Some researches have focused on the improvement of energy-efficiency of the hydraulic-valve-controlled systems [2-6]. However, it is still lower than that of the hydraulic pump-controlled system [5-6]. Hydraulic pump-controlled systems have high energy efficiency. However, the conventional pump-controlled systems that are altered by displacement have lower response. Recently, high response pump-controlled systems driven by AC servo motors are introduced [7-10]. The investigations on high response and high efficiency pump-controlled systems are still in progress.

This paper aims to investigate the servo performance of the high response and high energy efficiency electro-hydraulic pump-controlled system driven by a variable rotational speed AC servo motor in comparison with the conventional pump-controlled systems which are altered by displacement via variable displacement pumps. For that, the control strategy, adaptive fuzzy sliding-mode controller (AFSMC) is introduced. The AFSMC can not only simplify the fuzzy rule base but also estimate the equivalent control force and online self-tune the rule base through the adaptive strategy. The AC servo motor driving variable rotational speed pump-controlled system (VRSPCS) and the variable displacement pump-controlled system (VDPCS) controlled by AFSMC are implemented and verified experimentally for velocity control under external loading condition. Furthermore, the energy efficiencies of the experiments are analyzed and compared precisely by the power quality recorder used to measure the electrical power consumed by the power supply systems.

THE LAYOUT OF EXPERIMENTAL SYSTEM

The test rig layout of the variable rotational speed pump-controlled system (VRSPCS) and the variable displacement pump-controlled system (VDPCS) shown in Fig.1 is set up for experimentally investigating the dynamic behaviors of the control system in this paper. The test rig can be divided into four subsystems, including the hydraulic servo cylinder system, the hydraulic power supply system, the disturbance system and the PC-based control system. The specifications of the main components are listed in Table 1.

The hydraulic servo cylinder system contains a double-rod symmetrical hydraulic cylinder fitted with a linear encoder with the resolution of 0.1 μm. The hydraulic power supply system of VRSPCS consists of a swash plate axial piston pump with constant displacement of 12 ml/rev and is driven by an AC servo motor. In the velocity control of the VRSPCS, the motion of the controlled cylinder is regulated directly by the volume flow of the constant displacement pump, i.e. the motion of the controlled cylinder is controlled directly by the rotational speed of the AC servo motor. Thus, the control input signals of the AC servo motor are given from the PC-based controller via a D/A converter and enlarged by a servo amplifier. On the other hand, the hydraulic power supply system of

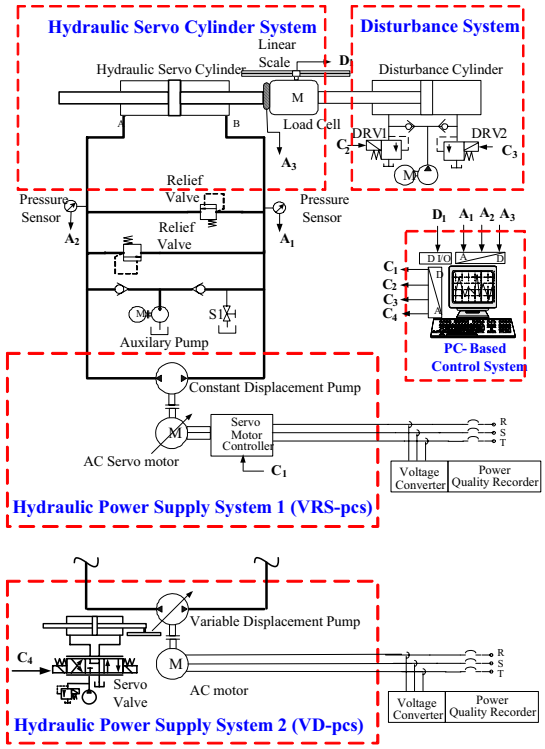

Figure 1 The layout of test rig

Table 1 Main components' specifications

Components	Specifications
AC servo motor	3ψ 220V, 7.0kW Rated rotational speed: 2000 rpm
Hydraulic axial piston pump	Max. pressure: 40 MPa Fixed displacement: 12 ml/rev
Hydraulic servo cylinder	Max. stroke: 400mm Piston /Rod diameter: 80/45mm
Disturance cylinder	Max. stroke: 400mm Piston /Rod diameter: 80/45mm
Optical encoder	Range: 500 mm Resolution: 0,1 μm
Load cell	Range: 111kN/10V
PC-based controller	AMD K6-2 450/512MB
Power quality recorder	Max. sampling rate: 10K/sec A/D resolution: 12bit ±1LSB Freq. response: 25KHz

VDPCS consists of a swash plate axial piston pump with variable displacement, a swash plate control unit and an AC motor. The maximum displacement of the variable displacement pump is 12 ml/rev at rotational speed 1700rpm. The swash plate control unit alters the swash plate's angle for changing the pump's displacement. The swash plate control unit contains a small hydraulic valve-controlled cylinder system for adjusting the swash plate angle. In the velocity control of the VDPCS, the motion of the controlled cylinder is regulated directly by the volume flow of the variable displacement pump. Thus, the control input signals of the motion control are given from the PC-based controller to the servo valve of the swash plate control unit via a D/A converter.

The velocity signals are generated by the digital differential of position signals that are measured by the linear encoder and fed back to the PC-based controller. The force signal is measured by the load cell and fed back to the PC-based controller. The overall electrical power supplied to the electro-hydraulic pump-controlled system is measured by the power quality recorder for energy efficiency analysis and comparison. Besides, the disturbance system, including a disturbance cylinder, two relief valves and a gear pump, is used here to generate external disturbance forces, which can be determined by setting the pressure of the relief valves DRV1 and DRV2, for the different loading conditions of experiments.

CONTROL STRATEGY AND CONTROLLER DESIGN

Fuzzy sliding mode control

Hwang et al. [12] proposed the methods to design the fuzzy sliding-mode controller for a non-linear system with 2nd order where the error and the error change rate were used to synthesize fuzzy reasoning rules. However, the rule number was larger and did not give the mathematical expression. This paper adopts the sliding surface $S=0$ and extends it to the fuzzy sliding surface $\tilde{S}=\tilde{0}$, and make S be a linguistic description of $\tilde{S}$. The fuzzy rules are given in the following form

$$R^l: \text{IF } S \text{ is } \tilde{F}_s^l \text{ THEN } u_{fs} \text{ is } \tilde{F}_u^{8-l},\ l=1,...,7. \tag{1}$$

According to the sup-min compositional rule of inference and the defuzzification accomplished by the center-of-area method, the mathematical expression can be derived as

$$u_{fs}=\begin{cases} 1 & ,if \quad z<-1 \\ \dfrac{7.5z^2+13.5z+5}{9z^2+15z+5} & ,if \quad -1\le z<-\dfrac{2}{3} \\ \dfrac{9z^2+11z+2}{18z^2+18z+2} & ,if \quad -\dfrac{2}{3}\le z<-\dfrac{1}{3} \\ \dfrac{1.5z^2+1.5z}{9z^2+3z-1} & ,if \quad -\dfrac{1}{3}\le z<0 \\ \dfrac{-1.5z^2+1.5z}{9z^2-3z-1} & ,if \quad 0\le z<\dfrac{1}{3} \\ \dfrac{-9z^2+11z-2}{18z^2-18z+2} & ,if \quad \dfrac{1}{3}\le z<\dfrac{2}{3} \\ \dfrac{-7.5z^2+13.5z-5}{9z^2-15z+5} & ,if \quad \dfrac{2}{3}\le z<1 \\ -1 & ,if \quad z\ge 1 \end{cases} \tag{2}$$

where $z=\dfrac{S}{\Phi}$, and when $|S|\ge\Phi$, it is easy to check $u_{fs}=-\mathrm{sgn}(S)$

Adaptive fuzzy sliding-mode controller

The state equations of the pump-controlled system model can be achieved as follows

$$\begin{aligned} \dot{x}_1 &= \dot{x}_p(t) \\ \dot{x}_1 &= x_2(t) \\ \dot{x}_2 &= -\sum_1^2 a_i x_i(t)+g(\underline{x})u+d(\underline{x})=f(\underline{x})+g(\underline{x})u+d(\underline{x}) \end{aligned} \tag{3}$$

in which $f(\underline{x})$ is the dynamic function of the pump-controlled system, $g(\underline{x})$ is a constant with positive value, and $d(\underline{x})$ is the disturbance function. Define the tracking error $e(t)$ as

$$e(t)=\dot{x}_d(t)-\dot{x}_p(t) \tag{4}$$

where $\dot{x}_p(t)$ indicates the control output and $\dot{x}_d(t)$ is the velocity target. Define a sliding surface as

$$S(t)=\dot{e}(t)+k_1 e(t) \tag{5}$$

Where k_1 is non-zero positive constants. Assume that parameters in Eq. (3) are well known and the external disturbance is measurable, then the control law can be derived as

$$u^*=g^{-1}(\underline{x})[\eta S_\Delta(t)-f(\underline{x})-d(\underline{x})+\ddot{x}_d+k_1\dot{e}(t)] \tag{6}$$

where $S_\Delta(t)=S(t)-\Phi\,\mathrm{sat}(S(t)/\Phi)$ and Φ is the boundary layer width of sliding surface S. The

properties of the function S_Δ are described as below in the design of adaptive law [11].

Property 1: As $|S| > \Phi, \Rightarrow |S_\Delta| = |S| - \Phi$ and $\dot{S}_\Delta = \dot{S}$.

Property 2: As $|S| \le \Phi, \ \Rightarrow \ S_\Delta = \dot{S}_\Delta = 0.$

Differentiate Eq. (5) as

$$\dot{S}(t) = -f(\underline{x}) - g(\underline{x})u - d(\underline{x}) + \ddot{x}_d + k_1 \dot{e}(t) \tag{7}$$

Substituting Eq. (6) into Eq. (7) gives

$$\dot{S}(t) + \eta S_\Delta(t) = 0, \qquad \eta > 0. \tag{8}$$

Eq. (8) shows that $\underline{e}(t) = [e(t), \dot{e}(t)]$ will converge to the neighbourhood of zero as $t \to \infty$, and the value of the neighbourhood depends on the value of Φ. However, the system parameters may be unknown or perturbed; the controller u^* cannot be precisely implemented. Therefore, by the universal approximation theorem, for any $\rho^* > 0$, an optimal fuzzy control $\hat{u}_{fz}(S, \underline{\alpha}^*)$ exists that satisfies

$$\left| u^* - \hat{u}_{fz}(S, \underline{\hat{\alpha}}^*) \right| \le \rho^* \tag{9}$$

where ρ^* is assumed to be bounded by $|\rho^*| \le M_\rho$. Utilize a fuzzy controller $\hat{u}_{fz}(S, \underline{\hat{\alpha}})$ to approximate u^* as

$$\hat{u}_{fz}(S, \underline{\hat{\alpha}}) = \underline{\hat{\alpha}}^T \underline{\xi} \tag{10}$$

where $\underline{\hat{\alpha}}$ is the estimated values of $\underline{\alpha}^*$. The control law for the developed adaptive fuzzy sliding-mode controller (AFSMC) is defined as the following form:

$$u = \hat{u}_{fz}(S, \underline{\hat{\alpha}}) + u_{comp}(S) \tag{11}$$

where the fuzzy controller $\hat{u}_{fz}$ is designed to approximate the controller u^* and the fuzzy sliding-mode compensation u_{comp} is proposed to compensate the difference between the controller u^* and fuzzy controller $\hat{u}_{fz}(S, \underline{\hat{\alpha}})$. Through Eqs. (6), (7) and (11), the dynamic equation can be derived as:

$$\dot{S}(t) + \eta S_\Delta(t) = g[u^* - \hat{u}_{fz}(\mathrm{S}, \underline{\hat{\alpha}}) - u_{comp}(S)] \tag{12}$$

For ensuring convergence to the boundary layer, the adaptive laws of the AFSMC are chosen as

$$\dot{\underline{\hat{\alpha}}} = \eta_1 \cdot S_\Delta \cdot \xi(S) \tag{13}$$

$$u_{comp}(S) = -\hat{\rho} \cdot u_{fs} \tag{14}$$

$$\dot{\hat{\rho}} = \eta_2 \cdot |S_\Delta| \tag{15}$$

Controller Design

The proposed AFSMC strategy will be implemented experimentally for the velocity control of the pump-controlled system through choosing the suitable control parameters g_s, g_u, the parameters k_1 in the sliding surface and the learning rate parameters (η_1, η_2).

EXPERIMENTS

Velocity control for velocity target 90mm/s

The velocity controls of the VRSPCS and VDPCS are implemented experimentally using AFSMC for velocity target 90mm/s with constant external loading force of 30 kN. Fig.2 indicates the experiment results of the velocity control response and the control error. The rising time of the velocity responses in VRSPC can reach 0.298 sec, and the settling time can be controlled within 0.438 sec. However, the rising time of the velocity responses in VDPCS is 0.375 sec, and the settling time is 0.654 sec. Furthermore, the transient state in VRSPCS is more stable compare to that in VDPCS. Thus, the high response performance in the VRSPCS is verified. Fig.2(b) schematically depicts the zoom in of the steady-state errors that can be controlled within 0.31 mm/s in the VRSPCS and within 0.25 mm/s in the VDPCS respectively. The excellent performance on velocity control accuracy can be clarified in the VRSPCS and VDPCS. The comparison of performance, including the rising time, the settling time and the steady state error is summarized in Table 2.

Energy efficiency in the velocity control

The power consumption in the experiment of velocity control, as shown in the above paragraph, is discussed in this section. The overall electrical power P_{in} supplied to the electro-hydraulic pump-controlled system is directly measured by the power quality recorder. The output power P_{out} of the controlled cylinder can be described as

$$P_{out} = F \cdot \dot{x} \tag{16}$$

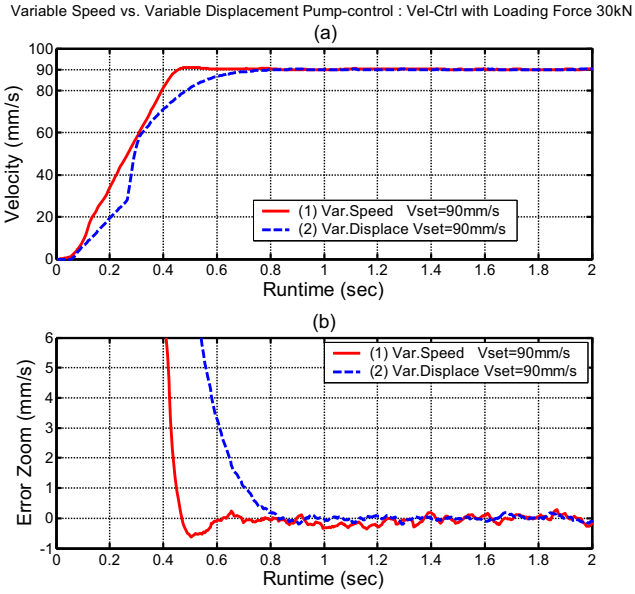

Figure 2 Experimental results of velocity control for velocity target 90mm/s under loading force 30kN in VRSPCS and VDPCS:(a) velocity control response (b) control error

Table 2 Comparison of velocity control performance for the velocity targets 90mm/s in VRPCS and VDPCS

Targets	VRSPCS	VDPCS
Rising time t_r (10~90%)	0.298 sec	0.375 sec
Settling time t_s (e < 2%)	0.438 sec	0.654 sec
Steady state error e_{ss}	0.31mm/s (0.34%)	0.25mm/s (0.27%)

where F and $\dot{x}$ are the output force and velocity of the controlled cylinder respectively. The output force is directly measured by the load cell, as shown in Fig.3. The feedback velocity signals are generated by the digital differential of position signal measured by the linear encoder. The supply power P_{in} and the output power P_{out} for the velocity control of 90 mm/s in the VRSPCS and VDPCS are shown in Fig.4(a) and Fig.4 (b) respectively. It is clear that the supply power is much less in the VRSPCS than in the VDPCS. The energy efficiency in the stead state can reach over 80% in the VRSPCS and can reach about 55% in the VDPCS, as shown in Fig.5. Consequently, the performance of high energy efficiency of the VRSPCS is evidenced.

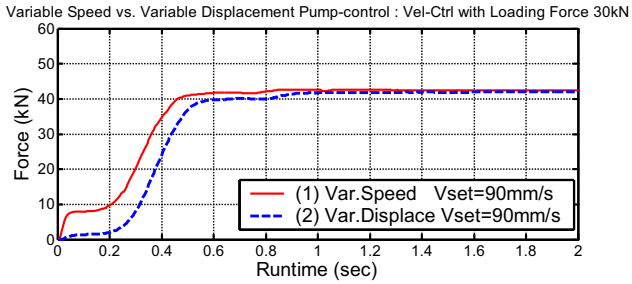

Figure 3 Output forces in the experiments of velocity control for velocity target 90mm/s under loading force 30kN in VRSPCS and VDPCS

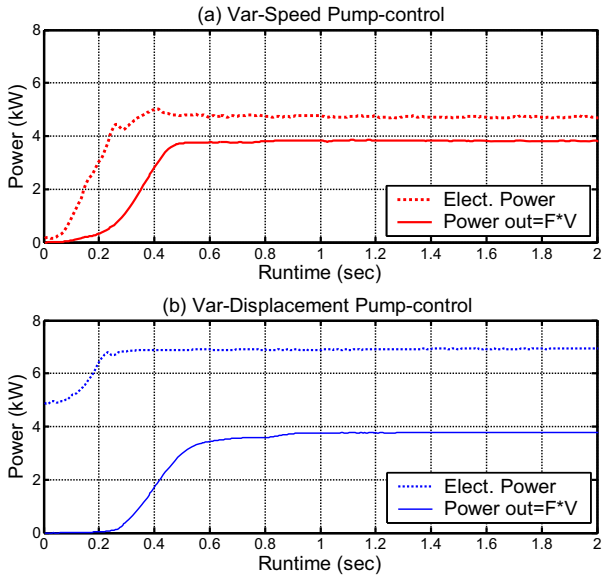

Figure 4 Supply power and output power in the experiments of velocity control for velocity target 90mm/s under loading force 30kN in VRSPCS and VDPCS.

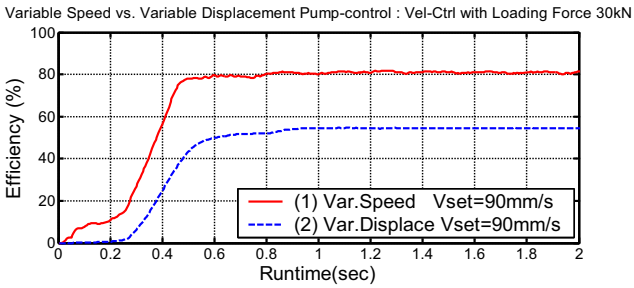

Figure 5 Energy efficiency in the experiments of velocity control for velocity target 90mm/s under loading force 30kN in VRSPCS and VDPCS.

CONCLUSIONS

1. This investigation developed a new electro-hydraulic pump-controlled system driven by the AC servo motor and axial piston pump for realizing velocity control with both high response and high energy-efficiency instead of the conventional variable displacement pump-controlled systems. For achieving better velocity control performance, adaptive fuzzy sliding-mode controller is used. The experimental results show that the VRSPCS realizes the performance of high response and little steady-state error.

2. The comparison of the velocity control performance and the energy efficiency measured by the power quality recorder used to measure the electrical power consumed are implemented. The energy efficiency of the VRSPCS in the velocity control for velocity target 90 mm/s under external loading force 30kN can achieves over 80%. It is evident that the VRSPCS realizes the performance of high energy efficiency.

ACKNOWLEDGEMENT

This research was supported by the National Science Council of Taiwan under the grant NSC 93-2212-E-011-036 and NSC 94-2212-E-011-019.

REFERENCES

1. Murrenhoff H, “Servohydrualik” (in German), Lecture notes, RWTH Aachen University, Germany, (1998).

2. Backé, W and Feigel H-J, “Neue Möglichkeiten beim Electro-hydraulischen Load-Sensing” (in German), O+P Ölhydraulik und Pneumatik 34, No.2, (1990), pp. 106-114.

3. Esders H, “Elektrohydraulisches Load-Sensing für Mobile Anwendungen”, (in German), O+P Ölhydraulik und Pneumatik 36, Nr.8, (1994), pp.473-480.

4. Kim S-D, Cho H-S and Lee C-O, “Stability Analysis of a Load-Sensing Hydraulic System”, Proc. of the Institute of Mechanical Engineers, Part A: Power and Process Engineering, Vol.202, No.A2, (1988), pp.79-88.

5.Chiang M-H and Chien Y-W, “Parallel control of velocity control and energy-saving control on a hydraulic valve controlled system using self-organizing fuzzy sliding mode control”, JSME International Journal, Series C, Vol.46, No.1, (2003), pp.224-231.

6.Chiang M-H, Lee L-W, Tsai J-J, “Concurrent implementation of high velocity control performance and high energy-efficiency for hydraulic injection moulding machines”, International Journal of Advanced Manufacturing Technology, 23, (2004), pp.256–262.

7. Bildstein A, “Application of electro-hydrostatic actuators (EHA) for future aircraft primary flight control”, Proc. of the 1. International Fluid Power Conference (1.IFK), Aachen, Germany, Band 1, (1998), pp.93-105.

8. Helduser S, “Electric-hydrostatic drive – an innovative energy-saving power and motion control system”, Proc. of Institution of Mechanical Engineers, Vol. 213, Part I, (1999), pp.427-439.

9. Habibi S and Goldenberg A, “Design of a new high performance electro-hydraulic actuator”, Proc. of the 1999 IEEE/ASME International Conference on Advanced Mechatroics, Atlanta, USA, (1999), pp.227-232.

10. Helbig A, “Injection moulding machine with electric-hydrostatic drives”, Proc. of the 3. International Fluid Power Conference (3. IFK), Aachen, Germany, Vol.1, (2002), pp.67-82.

11. R. M. Sanner, J. J. Slotine, “Gaussian Network for Direct Adaptive Control”, IEEE Trans. Neural Networks., vol. 3, pp. 837-863, 1992.

12.G. C. Hwang, S. Chang, “A Stability Approach to Fuzzy Control Design for Nonlinear System”, Fuzzy Sets Syst., vol. 48, pp.279–287, 1992.